Available online at www.sciencedirect.com
SCIENCE DIRECT
Journal of Photochemistry and Photobiology A: Chemistry 181 (2006) 120–125
Journal of Photochemistry and Photobiology A:Chemistry
www.elsevier.com/locate/jphotochem

Photocatalytic degradation of ethyl violet in aqueous solution mediated by TiO_2 suspensions

Chiing-Chang Chen [a,*], Chung-Shin Lu [a], Ying-Chien Chung [b]

[a] *Department of General Education, National Taichung Nursing College, Taichung 403, Taiwan, ROC*
[b] *Department of Biological Science and Technology, China Institute of Technology, Taipei 115, Taiwan, ROC*

Received 24 August 2005; received in revised form 13 October 2005; accepted 13 November 2005
Available online 20 December 2005

Abstract

The photodegradation of dye pollutants under visible light irradiation in TiO_2 dispersions continues to draw considerable attention because of the improving effective utilization of cost free solar energy and its potential application in treating wastewater from textile and photographic industries. To get a better understanding of the mechanistic details of this TiO_2-assisted photodegradation of the ethyl violet dye (EV, *N*,*N*,*N*′,*N*′,*N*″,*N*″-hexaethylpararosaniline) with visible light irradiation, the intermediates of the process were identified and examined by the HPLC-ESI-MS technique in this research. The analytical results indicated that seventeen intermediates were separated and identified. The experimental results indicated that the *N*-de-ethylation degradation of EV dye took place in a stepwise manner to yield mono-, di-, tri-, tetra-, penta-, hexa-*N*-de-ethylated EV species and, most of all, to yield *N*-hydroxyethylated intermediates, which were found for the first time in TiO_2-mediated photocatalysis process. The possible degradation pathways were proposed and discussed in this research. The reaction mechanisms of TiO_2/Vis proposed in this research would be useful for future application in the decoloration of dyes.

Keywords: Ethyl violet; Photodegradation; Titania; TiO_2; Photocatalytic

1. Introduction

Triphenylmethane dyes are used extensively in the textile industry for dyeing nylon, wool, cotton, and silk, as well as for coloring oil, fats, waxes, varnish, and plastics. The paper, leather, cosmetic, and food industries are also major consumers of various types of triphenylmethane dyes [1–3]. Additionally, these dyes are used as staining agents in bacteriological and histopathological applications. The photocytotoxicity of triphenylmethane dyes based on reactive oxygen species production is tested intensively with regard to their photodynamic therapy [4–7]. However, great concern regarding the thyroid peroxidase-catalyzed oxidation of the triphenylmethane class of dyes has arisen due to reactions which might form various *N*-de-alkylated primary and secondary aromatic amines, which have structures similar to aromatic amine carcinogens [8].

It is reported that 10–20% of dyes are lost to wastewater as a result of inefficiency in the dyeing process [2]. Dyestuffs from the textile and photographic industries are becoming a major source of environmental pollution. The large amount of dyestuffs used in the dyeing stage of textile manufacturing processes represents an increasing environmental danger due to their refractory carcinogenic nature [9]. To de-pollute the dyeing wastewater, a number of methods—including chemical oxidation and reduction, chemical precipitation and flocculation, photolysis, adsorption, ion pair extraction, electrochemical treatment and advanced oxidation—have been investigated [10]. Advanced oxidation is a promising technology for the clean up of dye-contaminated wastewaters due to its high removal efficiency. This technology is mainly based on oxidative reactions by $HO^{\bullet}$ radical generated by various methods such as O_3/UV, H_2O_2/UV, H_2O_2/Vis, O_3/H_2O_2/UV photolysis, photoassisted Fe^{3+}/H_2O_2, and TiO_2-mediated photocatalysis processes.

The TiO_2-mediated photocatalysis process has been successfully used to degrade dye pollutants during the past few years [11–17]. TiO_2 is broadly used as a photocatalyst because it is photochemically stable, nontoxic, and low cost [18–20]. The mechanism of dye degradation in the presence of TiO_2 particles irradiated by visible light is, however, different when compared

* Corresponding author. Tel.: +886 4 22196975.
E-mail address: ccchen@ntcnc.edu.tw (C.-C. Chen).

1010-6030/$ – see front matter © 2005 Elsevier B.V. All rights reserved.
doi:10.1016/j.jphotochem.2005.11.013

with UV light since the dyes are excited by the incident irradiation, and a successive electron injection from the excited dye to the conduction band of the semiconductor occurs, leaving the corresponding cationic dye radical. The dye radicals in turn react with the oxidizing radicals previously described and further degraded [21].

A possible reaction pathway(s) for the sensitized photodegradation of dyes in aqueous TiO_2 dispersions illuminated by visible irradiation was reported earlier [22–29]. The first photochemical step in the overall process, following the photoexcitation of dyes by visible light, is the formation of dye radical cations, $dye^{\bullet+}$ and generation of conduction band electrons (e_{cb}^-, usually taken to be surface Ti^{III} ions) or electrons trapped in surface states. This represents the charge separation process.

The electrons injected into the conduction band of the TiO_2 particles can either be scavenged by surface-adsorbed oxygen molecules to generate the superoxide radical anions $O_2^{\bullet-}$, or recombined with the $dye^{\bullet+}$ species. After the initial photochemical steps, a series of redox processes takes place involving the active radical species, $O_2^{\bullet-}$ or $^{\bullet}OH$, and the radical cations, $dye^{\bullet+}$, which will ultimately lead to the complete photoassisted degradation of the dye and its intermediates.

In earlier reports [11,23,28–29], the photodegradation of the triphenylmethane dyes were investigated. The *N*-de-alkylation process was predicated on the basis of the wavelength shift of maximal absorption of the dyes. However, only a portion of the *N*-de-alkylation intermediates of these dyes has been isolated and identified.

Therefore, this research focused on the identification of the reaction intermediates and understanding of the mechanistic details of the photodegradation of EV dye in the TiO_2/visible light process as a foundation for future application of this energy saving technology.

2. Experimental

2.1. Materials and reagents

Ethyl violet was obtained from Tokyo Kasei Kogyo Co. and used without any further purification. The chemical structure of ethyl violet is shown in Fig. 1. Stock solutions containing 1 g L^{-1} of EV in water were prepared, protected from light, and stored at 4 °C. HPLC analysis confirmed the presence of EV as a pure organic compound. The TiO_2 nanoparticles (P25, ca. 80% anatase, 20% rutile; particle size, ca. 20–30 nm; BET area, ca. 55 m^2 g^{-1}) were supplied by Degussa Co. and used in all the photocatalytic experiments.

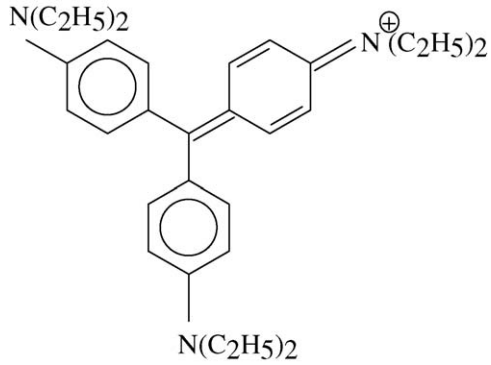

Fig. 1. Chemical structure of ethyl violet.

Reagent-grade ammonium acetate, nitric acid, sodium hydroxide and HPLC-grade methanol were purchased from Merck. De-ionized water was used throughout this study. The water was purified with a Milli-Q water ion-exchange system (Millipore Co.) to give a resistivity of 1.8×10^7 Ω cm.

2.2. Instruments

A Waters ZQ LC/MS system, equipped with a Waters 1525 Binary HPLC pump, a Waters 2996 Photodiode Array Detector, a Waters 717plus Autosampler, and a Waters micromass-ZQ4000 Detector was used. The reactor, a C-75 Chromato-Vue Cabinet of UVP, provides a wide area of illumination from the 15-W visible tubes positioned on two sides of the cabinet interior.

2.3. Photodegradation experiments

An aqueous TiO_2 dispersion was prepared by adding 50 mg of TiO_2 powder to a 100 mL solution containing the EV at appropriate concentrations. For reactions in different pH media, the initial pH of the suspensions was adjusted by addition of either NaOH or HNO_3 solutions. Prior to irradiation, the dispersions were magnetically stirred in the dark for ca. 30 min to ensure the establishment of an adsorption/desorption equilibrium. Irradiations were carried out using two visible lamps (15 W). At given irradiation time intervals, the dispersion was sampled (5 mL), centrifuged, and subsequently filtered through a Millipore filter (pore size, 0.22 μm) to separate the TiO_2 particles.

2.4. Procedures and analyses

After each irradiation cycle, the amount of residual dye was thus determined by HPLC. The analysis of organic intermediates was accomplished by HPLC-ESI-MS after readjustment of chromatographic conditions in order to make the mobile phase compatible with the working conditions of the mass spectrometer. Solvent A was 25 mM aqueous ammonium acetate buffer (pH 6.9), and solvent B was methanol. LC was carried out on an Atlantis^{TM} dC18 column (250 mm × 4.6 mm i.d., dp = 5 μm). The mobile phase flow rate was 1.0 mL min^{-1}. A linear gradient was run as follows: $t = 0$, $A = 95$, $B = 5$; $t = 20$, $A = 50$, $B = 50$; $t = 35$–40, $A = 10$, $B = 90$; $t = 45$, $A = 95$, $B = 5$. The column effluent was introduced into the ESI source of the mass spectrometer.

The quadruple mass spectrometer, equipped with an ESI interface with heated nebulizer probe at 350 °C, was used with an ion source temperature of 80 °C. ESI was carried out with the vaporizer at 350 °C, and nitrogen was used as sheath (80 psi) and auxiliary (20 psi) gas to assist with the preliminary nebulization and to initiate the ionization process. A discharge current of 5 μA was applied. Tube lens and capillary voltages were optimized for maximum response during the perfusion of the EV standard.

Blank experiments performed in flask without addition of TiO_2 show appreciable decolorization of the irradiated solution, thus confirming the expected good stability of this EV dye under visible irradiation. Addition of 0.5 g L^{-1} TiO_2 to solutions containing 50 mg L^{-1} of EVdid not alter the stability of the dye in the dark.

3. Results and discussion

The aqueous solutions of the EV dye were fairly stable to visible irradiation in absence of TiO_2. However, the EV can be degraded efficiently in aqueous TiO_2 dispersions by visible light irradiation. The UV–vis spectra changes during the photodegradation of EV in the aqueous TiO_2 dispersions under visible light irradiation are illustrated in Fig. 2. After irradiation for 68 h, ca. 99% of EV was degraded, the maximum absorption wavelength of the dye solution shifted from 592.0 to 560.7 nm. During visible irradiation, the characteristic absorption band of the dye around 592.0 nm decreased rapidly and shifted to lower wavelength (560.7 nm), but no new absorption bands appeared even in the ultraviolet range ($\lambda > 200$ nm). These results indicated that a series of *N*-de-ethylated intermediates may have formed and the whole conjugated chromophore structure of EV may have been cleaved. Similar phenomena were also observed during the photodegradation of sulforhodamine-B [11] and rhodamine-B [23] under visible irradiation.

Temporal variations occurring in the EV dye solution during the photodegradation with visible irradiation were examined by HPLC using a photodiode array detector and ESI mass spectrometry. The intermediates in the chromatogram recorded at 580 nm are illustrated in Fig. 3. Eighteen components (A–J, A′–F′, B″ and C″) are observed at retention time less than 55 min and for up to 60 h of irradiation. Except for the initial EV dye (peak A), the other peaks appear at 60 h of irradiation, indicating formation and transformation of the intermediates. The *N*-de-ethylation of the *N*,*N*,*N*′,*N*′,*N*″,*N*″-hexaethylpararosaniline (EV) has the wavelength position of its major absorption band moved toward the blue region, λ_{max}, EV, 592.0 nm; *N*,*N*-diethyl-*N*′,*N*′-diethyl-*N*″-ethylpararosaniline, 584.7 nm; *N*,*N*-diethyl-*N*′,*N*′-diethylpararosaniline, 577.3 nm; *N*,*N*-diethyl-*N*′-ethyl-*N*″-ethylpararosaniline, 577.5 nm; *N*,*N*-diethyl-*N*′-ethyl-pararosaniline, 576.1 nm; *N*-ethyl-*N*′-ethyl-*N*″-ethylpararosaniline, 576.7 nm; *N*,*N*-diethylpararosaniline, 565.1 nm; *N*-ethyl-*N*′-ethylpararosaniline, 571.2 nm; *N*-ethylpararosaniline, 556.6 nm; pararosaniline, 544.4 nm; *N*,*N*-diethyl-*N*′,*N*′-diethyl-*N*″-hydroxyethyl-*N*″-ethylpararosaniline, 616.5 nm; *N*,*N*-diethyl-*N*′-hydroxyethyl-*N*′-ethyl-*N*″-ethylpararosaniline, 584.7 nm; *N*,*N*-diethyl-*N*′,*N*′-diethyl-*N*″-hydroxyethylpararosaniline, 593.2 nm; *N*-hydroxyethyl-*N*-ethyl-*N*′-ethyl-*N*″-ethylpararosaniline, 576.1 nm; *N*,*N*-diethyl-*N*′-ethyl-*N*″-hydroxyethylpararosaniline, 593.2 nm; *N*,*N*-diethyl-*N*′-hydroxyethyl-*N*′-ethylpararosaniline, 584.7 nm; *N*-diethyl-*N*′-ethyl-*N*″-hydroxyethylpararosaniline, 565.4 nm; *N*-hydroxyethyl-*N*-ethyl-*N*′-ethylpararosaniline, 573.7 nm. The absorption maximum of the spectral bands also shifts from 592.0 nm (peak A) to 544.4 nm (peak J) and 609.1 nm (peak A′) to 565.4 nm (peak E′). This wavelength shift of the absorption band is presumed to result from the formation of a series of *N*-de-ethylated intermediates in a stepwise manner. Further irradiation caused the decrease of the absorption band at 544.4 nm, but no further wavelength shift was observed, implying that the band at 544.4 nm is that of the full *N*-de-ethylated product of EV dye. The wavelength shift is caused by *N*-de-ethylation because of attack by one of the active oxygen species on the *N*-ethyl group. The earlier work on the RhB/CdS system [30] inferred a primary step, in which the electron from the singlet excited state $^1RhB^*$ to CdS particles came from the nitrogen atoms. Moreover, in Fig. 4b, the hypsochromic shift of the absorption band is surmised to result from the formation of series of *N*-hydroxyethylated intermediates in a stepwise manner.

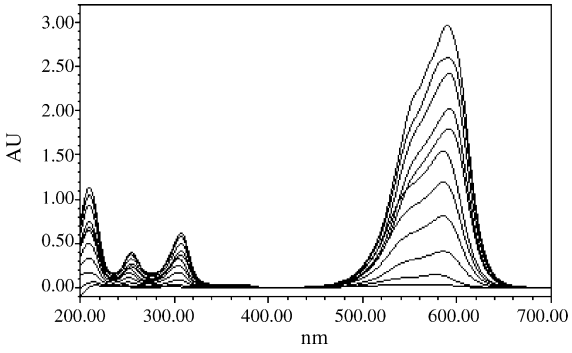

Fig. 2. UV–vis spectra change of EV in aqueous TiO_2 dispersions (EV: 50 mg L^{-1}, TiO_2: 0.5 g L^{-1}, pH 6) as a function of irradiation time. Spectra from top to bottom correspond to irradiation times of 4, 8, 16, 24, 36, 40, 52, 60, 68, 76, 84 h, respectively.

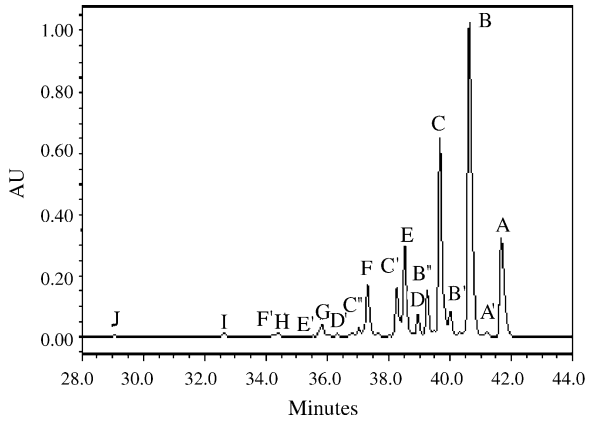

Fig. 3. HPLC chromatogram of the *N*-de-ethylated intermediates at 60 h of irradiation.

The *N*-de-ethylated intermediates were further identified using the HPLC-ESI mass spectrometric method. The molecular ion peaks appeared in the acid forms of the intermediates. From the results of mass spectral analysis, we confirmed that the component A, $m/z = 456.29$, in liquid chromatogram is EV. The other components are B, $m/z = 428.32$, *N*,*N*-diethyl-*N*′,*N*′-ethyl-*N*″-ethylpararosaniline; C, $m/z = 400.22$, *N*,*N*-diethyl-*N*′-ethyl-*N*″-ethylpararosaniline; D, $m/z = 400.22$, *N*,*N*-diethyl-*N*′,*N*′-diethylpararosaniline; E, $m/z = 372.12$, *N*-ethyl-*N*′-ethyl-*N*″-ethylpararosaniline; F, $m/z = 372.18$, *N*,*N*-diethyl-*N*′-ethylpararosaniline; G, $m/z = 344.15$, *N*-ethyl-*N*′-ethylpararo-

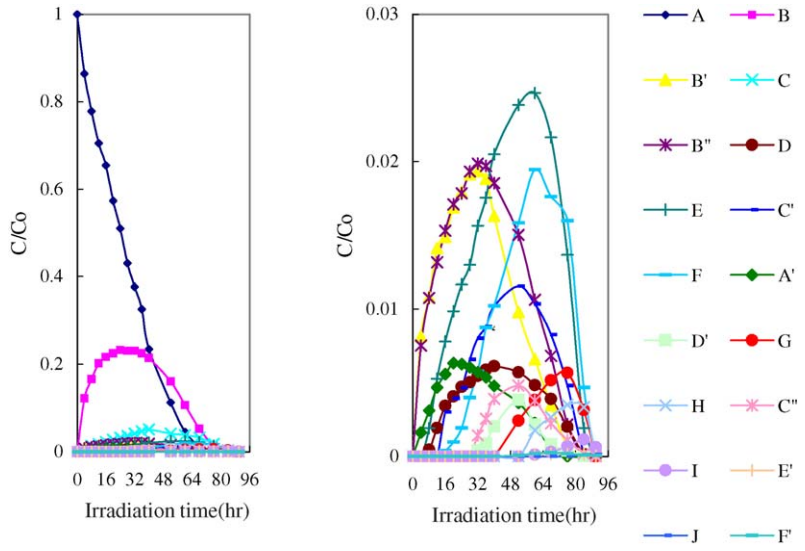

Fig. 4. Variation in the relative distribution of the *N*-de-ethylated products obtained from the photodegradation of EV as a function of irradiation time. Curves A–J and A′–F′ correspond to the peaks A–J and A′–F′ in the Fig. 3, respectively.

saniline; H, $m/z = 344.15$, *N*,*N*-diethylpararosaniline; I, $m/z = 316.11$, *N*-ethylpararosaniline; J, $m/z = 288.01$, pararosaniline; A′, $m/z = 472.29$, *N*,*N*-diethyl-*N*′,*N*′-diethyl-*N*″-hydroxyethyl-*N*″-ethylpararosaniline; B′, $m/z = 444.26$, *N*,*N*-diethyl-*N*′-hydroxyethyl-*N*′-ethyl-*N*″-ethylpararosaniline; B″, $m/z = 444.19$, *N*,*N*-diethyl-*N*′,*N*′-ethyl-*N*″-hydroxyethylpararosaniline; C′, $m/z = 416.16$, *N*-hydroxyethyl-*N*-ethyl-*N*′-ethyl-*N*″-ethylpararosaniline; C″, $m/z = 416.16$, *N*,*N*-diethyl-*N*′-ethyl-*N*″-hydroxyethylpararosaniline; D′, $m/z = 416.22$, *N*,*N*-diethyl-*N*′-hydroxyethyl-*N*′-ethylpararosaniline; E′, $m/z = 388.12$, *N*-ethyl-*N*′-ethyl-*N*″-hydroxyethylpararosaniline; and F′, $m/z = 388.19$, *N*′-hydroxyethyl-*N*′ethyl-*N*′-ethylpararosaniline. Results of HPLC chromatograms, UV–vis spectra, and HPLC-ESI mass spectra are summarized in Table 1.

These species correspond to the intermediates that possess from two to four fewer ethyl groups relative to the EV dye and are correlative with three pairs of isomeric molecules. One of these isomers, DMMPR, is formed by removal of an ethyl group from two different sides of the EV molecule while the other isomer in this pair, DDPR, is produced by removal of two ethyl groups from the same side of the EV structure. In the second pair of isomers, EEEPR is formed by removal of an ethyl group from each side of the EV molecule, and the other, DEPR, is produced by removal of both two ethyl groups from the same side of the EV structure and an ethyl group from the other side of the EV structure. In the third pair of isomers, DPR, is formed by removal of two ethyl groups from two different sides of the EV molecule while EEPR, is produced by removal of two ethyl groups from the same side of the EV structure and of an ethyl group from the rest of two sides of the EV structure. Both intermediates display identical HPLC-ESI-MS characteristics. Considering that the polarity of the DDPR, DEPR, and DPR

Table 1
Identification of the intermediates from the photodegradation of EV by HPLC-ESI-MS

HPLC peaks	*N*-de-ethylation intermediates	Abbreviation	ESI-MS peaks (*m*/*z*)	Absorption maximum (nm)
A	*N*,*N*,*N*′,*N*′,*N*″,*N*″-Hexaethylpararosani line	EV	456.29	592.0
B	*N*,*N*-Diethyl-*N*′,*N*″-diethyl-*N*′-ethylpararosaniline	DDEPR	428.25	584.7
C	*N*,*N*-Diethyl-*N*′-ethyl-*N*″-ethylpararos aniline	DEEPR	400.22	577.3
D	*N*,*N*-Diethyl-*N*′-diethylpararosaniline	DDPR	400.22	577.5
E	*N*-Ethyl-*N*′-ethyl-*N*″-ethylpararosaniline	EEEPR	372.12	576.1
F	*N*,*N*-Diethyl-*N*′-ethylpararosaniline	DEPR	372.18	576.7
G	*N*-Ethy-*N*′-ethylpararosaniline	EEPR	344.15	565.1
H	*N*,*N*-Diethylpararosaniline	DPR	344.15	571.2
I	*N*-Ethylpararosaniline	EPR	316.11	556.6
J	Pararosaniline	PR	288.01	544.4
A′	*N*,*N*-Diethyl-*N*′,*N*′-diethyl-*N*″-hydroxyethyl-*N*″-ethylpararosaniline	DDHEPR	472.29	616.5
B′	*N*,*N*-Diethyl-*N*′-hydroxyethyl-*N*′-ethyl-*N*″-ethylpararosaniline	DHEEPR	444.26	584.7
B″	*N*,*N*-Diethyl-*N*′,*N*′-ethyl-*N*″-hydroxyethylpararosaniline	DDHPR	444.19	593.2
C′	*N*-Hydroxyethyl-*N*-ethyl-*N*′-ethyl-*N*″-ethylpararosaniline	HEEEPR	416.16	576.1
C″	*N*,*N*-Diethyl-*N*′-ethyl-*N*″-hydroxyethylpararosaniline	DMHPR	416.16	593.2
D′	*N*,*N*-Diethyl-*N*′-hydroxyethyl-*N*″-ethylpararosaniline	DHEPR	416.22	584.7
E′	*N*-Ethyl-*N*′-ethyl-*N*″-hydroxyethylpararosaniline	EEHPR	388.12	565.4
F′	*N*-Hydroxyethyl-*N*-ethyl-*N*′-ethylpararosaniline	HEEPR	388.19	573.7

species exceeds that of the DEEPR, EEEPR and EEPR intermediates, we expected the latter to be eluted after the DDPR, DEPR and DPR species. Additionally, to the extent that two *N*-ethyl groups are stronger auxochromic moieties than either the *N*,*N*-diethyl or amino groups, the maximal absorption of the DDPR, DEPR and DPR intermediates was anticipated to occur at wavelengths shorter than the band position of the DEEPR, EEEPR and EEPR species. The following results and the proposed mechanism support this argument.

The relative distribution of all of the *N*-de-ethylated intermediates obtained is illustrated in Fig. 4. To minimize errors, the relative intensities were recorded at the maximum absorption wavelength for each intermediate although the complete quantitative determination of all of the photogenerated intermediates was not achieved, owing to unavailable appropriate molar extinction coefficients of these intermediates and unavailable reference standards. Nonetheless, we clearly observed the changes in the distribution of each intermediate during the photodegradation of EV.

Wu et al. [23] suggested that *N*-de-ethylation is caused by an attack of active oxygen species on the *N*-ethyl groups. The abundance of acetaldehyde in the reaction mixture supported that inference. The indispensable presence of molecular O_2 for both the degradation and the *N*-de-ethylation processes was additional evidence for that assertion. Unlike UV irradiation, under which most of the $^{\bullet}OH$ is generated directly from the reaction between the holes and surface-adsorbed H_2O or OH^-, the only pathway for the formation of reactive oxygen species under visible irradiation is through the reduction of O_2 by the conduction band electron. The probability for the formation of $^{\bullet}OH$ should be much lower than for that of $O_2^{\bullet-}$. De-ethylation of the EV dye occurs mostly through attack by the $O_2^{\bullet-}$ species, which is a perfect nucleophilic reagent, on the *N*-ethyl portion of EV. Additionally, considering that the *N*,*N*-diethyl group in DDPR, DEPR and DPR is bulkier than in the *N*-ethyl group in DEEPR, EEEPR and EEPR molecules, nucleophilic attack by $O_2^{\bullet-}$ on the *N*-ethyl group should be favored at the expense of the *N*,*N*-diethyl group. In accord with this notion, the HPLC results showed that the DDPR, DEPR, and DPR intermediates reached maximal concentration before the DEEPR, EEEPR, and EEPR intermediates did. However, considering that the attack probability of the two *N*,*N*-diethyl groups in DDEPR is higher than in the one *N*-ethyl group in DDEPR molecules, nucleophilic attack by $O_2^{\bullet-}$ on the *N*,*N*-diethyl group should be favored at the *N*-ethyl group. The *N*-di-de-ethylated intermediates (DEEPR and DDPR) were clearly observed (Fig. 4, curves C and D) that DEEPR and DDPR reached their maximum concentration at the same time after a 40-h irradiation period because of the two competitive factors mentioned above. The *N*-tri-de-ethylated intermediates (EEEPR and DEPR) were clearly observed (Fig. 4, curves E and F) that EEEPR reached its maximum concentration after a 60-h irradiation period while DEPR reached its maximum concentrations after 60 h because the $O_2^{\bullet-}$ attacked the *N*-ethyl group of DEEPR and the *N*,*N*-diethyl group of DDPR. The *N*-tetra-de-ethylated intermediates (EEPR and DPR) were clearly observed (Fig. 4, curves G and H) that EEPR reached its maximum concentration after a 76-h irradiation period because the $O_2^{\bullet-}$ attacked the *N*-ethyl group of EEEPR and the *N*,*N*-diethyl group of DEPR while DPR reached its maximum concentrations after a 76-h irradiation period because the $O_2^{\bullet-}$ attacked the *N*-ethyl group of DEPR. In the *N*-penta-de-ethylated intermediates (EPR) (Fig. 4, curve I), EPR reached its maximum concentration after an 84-h irradiation period because the $^{\bullet}OH$ attacked the *N*-ethyl group of EEPR and the *N*,*N*-diethyl group of DPR. In the *N*-hexa-de-ethylated intermediates (PR) (Fig. 4, curve J), PR reached its maximum concentration after a 90-h irradiation period. In the hydroxylation of *N*-hexa-ethylated intermediates (Fig. 4, curve A′), DDHEPR reached its maximum concentration after a 20-h irradiation period because the $O_2^{\bullet-}$ attacked the *N*,*N*-diethyl group of EV. In the hydroxylation of *N*-penta-ethylated intermediates (Fig. 4, curves B′ and B″), DHEEPR and DDHPR reached their maximum concentration after a 32-h irradiation period because the $O_2^{\bullet-}$ attacked the *N*,*N*-diethyl group of DDEPR and the *N*-ethyl group of DDEPR. In the hydroxylation of *N*-tetra-ethylated intermediates (Fig. 4, curves C′ and C″), HEEEPR and DEHPR reached their maximum concentration after a 52-h irradiation period because the $O_2^{\bullet-}$ attacked the *N*,*N*-diethyl group of DEEPR and the *N*-ethyl group of DEEPR. In the hydroxylation of *N*-tetra-ethylated intermediates (Fig. 4, curve D′), DHEPR reached its maximum concentration after a 52-h irradiation period because the $O_2^{\bullet-}$ attacked the *N*,*N*-diethyl group of DDPR. In the hydroxylation of *N*-tri-methylated intermediates (Fig. 4, curve E′), EEHPR reached its maximum concentration after a 68-h irradiation period because the $O_2^{\bullet-}$ attacked the *N*-ethyl group of EEEPR. In the hydroxylation of *N*-tri-methylated intermediates (Fig. 4, curve F′), HEEPR reached its maximum concentration after a 68-h irradiation period because the $O_2^{\bullet-}$ attacked the *N*,*N*-diethyl group of DEPR. The successive appearance of the maximal quantity of each intermediate indicates that the *N*-de-ethylation of EV is a stepwise photochemical process that occurs by a de-hydroxylation of *N*-hydroxyethylated intermediates.

The *N*-mono-de-ethylated intermediates (DDEPR) and *N*-di-de-ethylated intermediates (DDPR and DEEPR) were clearly observed (Fig. 4, curves B–D), and afterward DDEPR degraded rapidly. A small amount of the final *N*-de-ethylated intermediate (PR) was also detected (Fig. 4, curve J). The first product (DDEPR) of *N*-de-ethylation reached its maximum concentration after a 24-h irradiation period (Fig. 4, curve B) while the maximum of the final *N*-de-ethylated product (PR) appeared after irradiation for 96 h (Fig. 4, curve J). The chromophoric species (EV) was still apparent following irradiation for 96 h. This indicates that the *N*-de-ethylation process by hydroxylation predominates and that the cleavage of the conjugated structure occurs at a somewhat slower rate until all six-ethyl groups are removed.

According to earlier reports [31–32], most oxidative *N*-dealkylation processes are preceded by the formation of a nitrogen-centered radical while destruction of dye chromophore structures is preceded by generation of a carbon-centered radical [28,33]. If degradation of EV is consistent, it must occur via two different photooxidation pathways (destruction of the chromophore structure and *N*-de-ethylation) due to formation of different radicals (either a carbon-centered or nitrogen-centered

radical). There is no doubt that electron injection from the dye to the conduction band of TiO_2 yields dye cation radical, a process determined by the nature of the HOMO orbital of the excited dye, $^{1,3}dye^*$ [34]. After this step, the cation radical, $dye^{\bullet+}$, can undergo hydrolysis and/or deprotonation pathways of the dye cation radicals, which in turn are determined by the different adsorption modes of EV on the TiO_2 particle surface.

On the basis of all experimental results above, the dye molecule in the EV/TiO_2 system is adsorbed through the positively charged diethylamine function. Following electron injection from the TiO_2 particle surface to the adsorbed dye through the positively charged diethylamine function and subsequence hydrolysis (or deprotonation) yields a nitrogen-centered radical, which is subsequently attacked by molecular oxygen to lead ultimately to de-ethylation. The mono-de-ethylated dye, DDEPR, can also be adsorbed on the TiO_2 particle surface and be implicated in other similar events (electron injection, hydrolysis or deprotonation, and oxygen attack) to yield a bi-de-ethylated dye derivative, DDPR and DEEPR. The *N*-de-ethylation process described above continues until the completely *N*-de-ethylated dye, PR, is formed.

4. Conclusion

In the TiO_2-assisted photodegradation system, the *N*-de-ethylation process by hydroxylated intermediates predominates during the initial irradiation period, as first confirmed by HPLC-ESI-MS and UV–vis spectra. The *N*-de-ethylation of EV takes place in a stepwise manner with the various *N*-de-ethylated and hydroxylated intermediate EV species remaining in equilibrium between the TiO_2 surface and the bulk solution. The *N*-de-ethylation process described above continues until the completely *N*-de-ethylated dye is formed. The reaction mechanisms of TiO_2/Vis proposed in this research would be useful for future application to the decoloration of dyes. Besides, the ethyl groups are removed one by one as confirmed by the gradual peak wavelength shifts toward the blue region. The hypsochromic effects resulting from *N*-de-ethylated and hydroxylated intermediates of EV occurred concomitantly during irradiation.

References

[1] Ullmann's Encyclopedia of Industrial Chemistry. Part A27. Triarylmethane and Diarylmethane Dyes, sixth ed., Wiley-VCH, New York, 2001.
[2] H. Zollinger, Color Chemistry: Syntheses, Properties, and Applications of Organic Dyes and Pigments, second ed., VCH, Weinheim, 1991.
[3] R.L. Feller, Accelerated Aging. Photochemical and Thermal Aspects, The J. Paul Getty Trust, 1994.
[4] A.C. Bhasikuttan, A.V. Sapre, L.V. Shastri, J. Photochem. Photobiol. A: Chem. 150 (2002) 59–66.
[5] M.S. Baptista, G.L. Indig, J. Phys. Chem. B 102 (1998) 4678–4688.
[6] R. Bonnett, G. Martinez, Tetrahedron 57 (2001) 9513–9547.
[7] A.J. Kowaltowski, J. Turin, G.L. Indig, J. Bioenerg. Biomember 31 (1999) 581–590.
[8] B.P. Cho, T. Yang, L.R. Blankenship, J.D. Moody, M. Churchwell, F.A. Bebland, S.J. Culp, Chem. Res. Toxicol. 16 (2003) 285–294.
[9] A. Reife, Dyes environmental chemistry, in: Kirk. (Ed.), Othmer Encyclopedia of Chemical Technology, vol. 8, fourth ed., John Wiley & Sons Inc., New York, 1993, pp. 753–784.
[10] W. Azmi, R.K. Sani, U.C. Banerjee, Enzyme Microb. Technol. 22 (1998) 185–191.
[11] C.C. Chen, W. Zhao, J.G. Li, J.C. Zhao, H. Hidaka, N. Serpone, Environ. Sci. Technol. 36 (2002) 3604–3611.
[12] S. Parra, S.E. Stanca, I. Guasaquillo, K.R. Thampi, Appl. Catal. B: Environ. 51 (2004) 107–116.
[13] R. Asahi, T. Morikawa, T. Ohwaki, K. Aoki, Y. Taga, Science 293 (2001) 269–271.
[14] M. Karkmaz, E. Puzenat, C. Guillard, J.M. Herrmann, Appl. Catal. B: Environ. 51 (2004) 183–194.
[15] W. Chu, C.C. Wong, Environ. Sci. Technol. 37 (2003) 2310–2316.
[16] H. Hidaka, H. Honjo, S. Horikoshi, N. Serpone, New J. Chem. 27 (2003) 1371–1376.
[17] P. Lu, F. Wu, N.S. Deng, Appl. Catal. B: Environ. 53 (2004) 87–93.
[18] A.L. Linsebigler, J.T.Y. G.Q. Lu Jr., Chem. Rev. 95 (1995) 735–758.
[19] M.R. Hoffman, S.T. Martin, W. Choi, W. Bahnemann, Chem. Rev. 95 (1995) 69–96.
[20] C.C. Chen, X. Li, J. Zhau, H. Hidaka, N. Serpone, J. Phys. Chem. B 106 (2002) 318–324.
[21] P.V. Kamat, Langmuir 6 (1990) 512–513.
[22] T. Watanabe, T. Takizawa, K. Honda, J. Phys. Chem. 81 (1977) 1845–1851.
[23] T. Wu, G. Liu, J. Zhao, H. Hidaka, N. Serpone, J. Phys. Chem. B 102 (1998) 5845–5851.
[24] K. Vinodgopal, D.E. Wynkoop, P.V. Kamat, Environ. Sci. Technol. 30 (1996) 1660–1666.
[25] C. Nasr, K. Vinodgopal, L. Fisher, S. Hotchandani, A.K. Chattopadhyay, P.V. Kamat, J. Phys. Chem. 100 (1996) 8436–8442.
[26] T. Wu, T. Lin, J. Zhao, H. Hidaka, N. Serpone, Environ. Sci. Technol. 33 (1999) 1379–1387.
[27] Y. Cho, W. Choi, Environ. Sci. Technol. 35 (2001) 966–970.
[28] X. Li, G. Liu, J. Zhao, New J. Chem. 23 (1999) 1193–1196.
[29] M. Saquib, M. Muneer, Dyes Pigments 56 (2003) 37–49.
[30] C.C. Wong, W. Chu, Environ. Sci. Technol. 37 (2003) 2310–2316.
[31] B.L. Laube, M.R. Asirvatham, C.K. Mann, J. Org. Chem. 42 (1977) 670–674.
[32] F.C. Shaefer, W.D. Zimmermann, J. Org. Chem. 35 (1970) 2165–2174.
[33] G. Liu, J. Zhao, K. Wu, K. Oikawa, H. Hidaka, N. Serpone, Environ. Sci. Technol. 33 (1999) 2081–2087.
[34] G. Liu, X. Li, J. Zhao, H. Hidaka, N. Serpone, Environ. Sci. Technol. 34 (2000) 3982–3990.